 http://dx.doi.org/10.14500/aro.10041

Static Analysis of Steel Fiber Concrete Beam With Heterosis Finite Elements

James H. Haido

Department of Water Resources Engineering, Faculty of Engineering, University of Duhok
Duhok, Kurdistan Region - F.R. Iraq

***Abstract*— Steel fiber is considered as the most commonly used constructional fibers in concrete structures. The formulation of new nonlinearities to predict the static performance of steel fiber concrete composite structures is considered essential. Present study is devoted to investigate the efficiency of utilizing heterosis finite elements analysis in static analysis of steel fibrous beams. New and simple material nonlinearities are proposed and used in the formulation of these elements. A computer program coded in FORTRAN was developed to perform current finite element static analysis with considering four cases of elements stiffness matrix determination. The results are compared with the experimental data available in literature in terms of central deflections, strains, and failure form, good agreement was found. Suitable outcomes have been observed in present static analysis with using of tangential stiffness matrix and stiffness matrix in second iteration of the load increment.**

***Index Terms*—Hetrosis elements, mechanics of concrete structures, static analysis.**

I. Introduction

It is reality that, except of chemical and mineral admixtures, the mechanical properties of concrete are enhanced with introducing of different ingredients to the fresh concrete as steel fibers, carbon fibers, glass fibers etc. Recently, the using of steel fiber reinforced concrete SFRC is increased in real-life applications. SFRC is widely used in many constructions such as tunnels, beams and slabs, domes, reinforced concrete building to resist seismic actions and marine structures. The employing of special sizes of steel fibers in concrete material improves crack performance which produces a ductile concrete with good absorption capacity (Ocean Heidelberg Cement Group, 1999). The ductile analysis and design of reinforced concrete beams are usually considered in flexural problems.

Many experimental and numerical works have been launched to investigate the performance of SFRC beams under the effect of static loadings. The effect of steel fibers on beam flexural cracking, toughness of SFRC beams, shear resistance, crack width, static load capacity and compressive strength and tensile strength have been studied in many references (Dupont and Vandewalle, 2002; Gopalaratnam, et al., 1991; Paine et al., 2002; Ganesan and Shivananda, 2002; Alavizadeh-Farhang, 1998; Hartman, 1999; Compione and Mangiavillano, 2008; Cucchiara, et al., 2004).

Numerical procedures have been used to study the static behavior of SFRC beams by many authors (Bangash, 1989; Hemmaty, 1998; ANSYS, 2003; Huyse, et al., 1994).

Due to the fact that many shapes of steel fibers are available to use in concrete structures, the need for new and simple nonlinear relationships for mechanical properties of SFRC material is considered useful. Therefore, present endeavor is concentrated in developing new finite element procedure for static analysis of SFRC beams with introducing new simple nonlinear material formulations with heterosis elements.

II. Methodology

Current static analysis comprises of proposing new and simple nonlinearities and using them in producing a novel developed finite element procedure for concrete beam analysis with using heterosis nine-noded elements.

A. Heterosis Elements

In present investigation, the heterosis shell elements are used. These elements are characterized with three displacements and two rotations at each nodal point. The local coordinates (α, β) of each node are illustrated in Fig. 1.

The Cartesian coordinates (x, y and z) of any point over each element can be determined by using the nodal coordinate values (x_i, y_i and z_i) and nodal shape function N_i as follows:

$$\begin{Bmatrix} x \\ y \\ z \end{Bmatrix} = \sum_{i=1}^{n} N_i(\alpha,\beta).\begin{Bmatrix} x_i \\ y_i \\ z_i \end{Bmatrix} \quad (1)$$

ARO-The Scientific Journal of Koya University
Volume II, No(1)2014, Article ID: ARO.10041, 10 pages
DOI: 10.14500/aro.10041
Received 15 April 2014; Accepted 17 June 2014
Regular research paper: Published 25 August 2014
Corresponding author's e-mail: james.haido@uod.ac

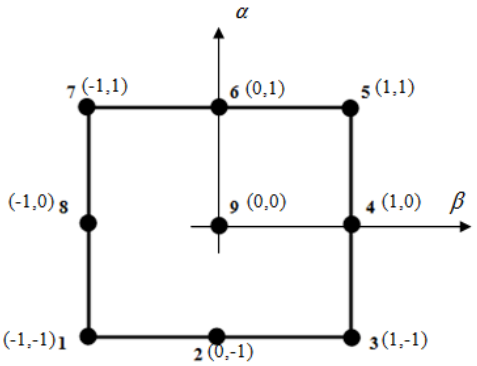

Fig. 1. Local coordinates of heterosis element.

In the similar manner, the displacement at any location (u, v, w) over the element can be estimated using the nodal displacements of u_i, v_i and w_i in x, y and z directions respectively of each element as hereunder:

$$\begin{Bmatrix} u \\ v \\ w \end{Bmatrix} = \sum_{i=1}^{n} N_i . \begin{Bmatrix} u_i \\ v_i \\ w_i \end{Bmatrix} \tag{2}$$

The displacements are determined at each nodal point, while the strains are found at each Gauss point. The element is separated into concrete and reinforcement steel bar plates through the beam depth. The Gauss points are located over each plate as in Fig. 2. The strain and stress values are determined at each Gauss point.

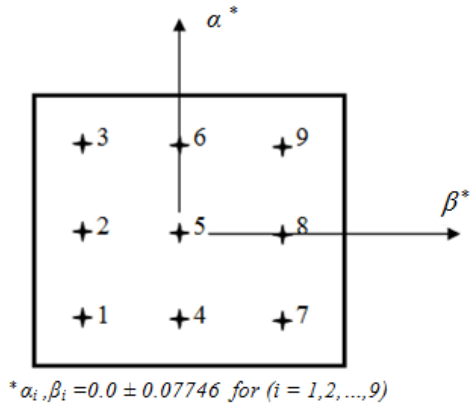

Fig. 2. Location of nine Gauss points of heterosis element.

The strain vector is given as (Al-Ta'an and Ezzadeen, 1995):

$$\{\varepsilon\} = [B]\{\delta\} \tag{3}$$

where; $\{\varepsilon\}$ is the nodal strain vector, $\{\delta\}$ is the nodal displacement vector and $[B]$ is the strain - displacement matrix which separated into two parts namely bending and shear displacement - strain matrices which are given as follows:

$$[B]_b = [B^1, B^2, B^3, ..., B^9] \tag{4}$$

$$B^i = \begin{bmatrix} 0 & \frac{\partial P_i}{\partial x} & 0 \\ 0 & 0 & \frac{\partial P_i}{\partial y} \\ 0 & \frac{\partial P_i}{\partial y} & \frac{\partial P_i}{\partial x} \end{bmatrix} \quad \text{for } 1 \le i \le 8 \tag{5}$$

And for node 9, B^i will be as follows:

$$B^9 = \begin{bmatrix} \frac{\partial P_9}{\partial x} & 0 \\ 0 & \frac{\partial P_9}{\partial y} \\ \frac{\partial P_9}{\partial y} & \frac{\partial P_9}{\partial x} \end{bmatrix} \tag{6}$$

$$[B]_s = [B_s^1, B_s^2, ..., B_s^9] \tag{7}$$

$$B_s^i = \begin{bmatrix} \frac{\partial N_i}{\partial x} & -P_i & 0 \\ \frac{\partial N_i}{\partial y} & 0 & -P_i \end{bmatrix} \quad \text{for } 1 \le i \le 8 \tag{8}$$

and

$$B_s^9 = \begin{bmatrix} -P_9 & 0 \\ 0 & P_9 \end{bmatrix} \quad \text{for node 9} \tag{9}$$

Where;
B_b^i is bending strain – displacement component for nodes i = 1 to 8, B_b^9 is bending strain – displacement component for node i = 9, P_i is Lagrangian shape function, B_s^i is shear strain – displacement component for nodes i = 1 to 8 and B_s^9 is shear strain – displacement component for node i = 9.

Consequently, the stiffness matrix [S] of each element is divided into two groups namely element stiffness matrix for bending [S_b] and element stiffness matrix for shear [S_s] as follows:

$$[S] = [S_b] + [S_s] \tag{10}$$

B. Present Nonlinear Relationships of SFRC Behavior

The introducing of steel fibers in concrete will lead to produce non-homogenous material which characterized by different behaviors under tension and compression actions. Thus, in order to simulate the performance of concrete material, suitable nonlinearities are required to represent the

concrete behavior under compression and tension forces in the finite element procedure (Abdul-Razzak and Ali, 2011a; Abdul-Razzak and Ali, 2011b).

Depending on theories of elasticity and plasticity, the compression behavior of concrete can be considered in finite element analysis. To simulate this compression behavior, Madrid equation was employed to represent the yield surface growing during the compression loading as follows (Al-Ta'an and Ezzadeen, 1995):

$$\sigma_c = -f_{co}\frac{\varepsilon_c}{\varepsilon_{cs}}\left[\frac{\varepsilon_c}{\varepsilon_{cs}}-2\right] \tag{11}$$

Where;
σ_c is the compression stress,
ε_c is the compression strain,
ε_{cs} and is the strain value corresponding to concrete compression strength,
f_{co} is the compression strength of concrete.

The modulus of elasticity of concrete Ec is given by the following formula:

$$E_c = \frac{2f_{co}}{\varepsilon_{cs}} \tag{12}$$

Therefore, (1) can be given as follows:

$$\sigma_c = E_c\varepsilon_c - \frac{E_c\varepsilon_c^2}{2\varepsilon_c} \tag{13}$$

The derivation of (13) with respect to ε_{cs} is named by hardening parameter Hp which is given as:

$$Hp = \left(\sqrt{\frac{\varepsilon_{cs}}{\varepsilon_{pl}}}-1\right) \tag{14}$$

where;

$$\varepsilon_{pl} = \varepsilon_c - \frac{\sigma_c}{E_c} \tag{15}$$

Hp is used in representing the growing of compression stress curve of SFRC.

In the case of steel fiber concrete material under two perpendicular compression forces, the concrete strength f_{c2} is increased by a value of magnification factor ir as follows:

$$f_{c2} = ir.f_{co} \tag{16}$$

where $ir \geq 1.0$

Depending on numerous experimental data in literature (Hsu and Hsu, 1994; Ashour, et al., 2000; Kurihara, et al., 2000; Bayramov, et al., 2004; Song and Hwang, 2004; Lim and Nawy, 2005; Koksal, et al., 2008; Thomas and Ramaswamy, 2007; Lin, et al., 2008; Bencardino, et al., 2010), the formula for magnification factor ir is proposed with using of nonlinear regression analysis of these experimental data in SPSS 17 program. Two parameters are considered in formulating ir equation namely fiber content Co and fiber aspect ratio A_f as follows:

$$ir = 1.997a \tag{17}$$

where

$$a = \sqrt{Co.Af} \tag{18}$$

$$Af = \frac{fiber\ \ length}{fiber\ \ equivalent\ \ diameter} \tag{19}$$

An expression is proposed also for ε_{cs} as hereunder:

$$\varepsilon_{cs} = 0.004628a \tag{20}$$

To predict the crushing at each Gauss point, the maximum compression strain value is represented in mathematical formulation depending on experimental data in aforementioned references as follows:

$$\varepsilon_{crush} = 0.009631a \tag{21}$$

In the current work, tension strain magnitude ε_{ts} corresponding to the tensile strength of SFRC material is used to predict the SFRC behavior under tension forces. The best formulation of this strain is proposed based on the nonlinear regression rule as follows:

$$\varepsilon_{ts} = 0.0002698a \tag{22}$$

The cracks are supposed to be formed at Gauss points, when the tension strain is reached the strain value ε_{ts}.

After occurring of cracks at Gauss point, the Poisson's ratio and modulus of elasticity are considered null in the perpendicular direction to the cracks. Then the reduced cracked modulus is employed to represent the aggregate interlock. The cracked modulus S_{cr} is determined according to the regression analysis of previously mentioned references (Hsu and Hsu, 1994; Ashour, et al., 2000; Kurihara, et al., 2000; Bayramov et al., 2004; Song and Hwang, 2004; Lim and Nawy, 2005; Koksal, et al., 2008; Thomas and Ramaswamy, 2007; Lin, et al., 2008; Bencardino, et al., 2010) as follows:

$$S_{cr} = 5.533a \tag{23}$$

Based on the present proposed strain value of ε_{ts}, two nonlinear equations given by Hasan (2002) are modified as hereunder:

$$\sigma_{tb} = f_{te}\left[1-\left((1-\frac{\varepsilon_{tb}}{\varepsilon_{ts}})\right)^{E_i.\frac{\varepsilon_{ts}}{f_{te}}}\right] \quad (24)$$

$$\sigma_{ta} = f_{te}.e^{-f_{te}.F.(\frac{\varepsilon_{ta}}{\varepsilon_{ts}}-1)^G} \quad (25)$$

Where;
σ_{tb} tensile stress before crack,
σ_{ta} tensile stress after crack,
Ei initial modulus of elasticity of SFRC based on the experimental tensile strength values used by Hasan (2002),
f_{te} concrete tensile strength,
ε_{tb} tensile strain before crack,
ε_{ta} tensile strain after crack.

$$F = 0.66875 - 0.48842\left(Co.\frac{fiber\ \ length}{fiber\ \ diameter}\right) + 0.1125\left(Co.\frac{fiber\ \ length}{fiber\ \ diameter}\right)^2 \quad (26)$$

$$G = 6.26513\left(\frac{fiber\ \ length}{Co.fiber\ \ diameter}\right)^{-0.50327} \quad (27)$$

These proposed nonlinear formulations can be given graphically with using common values of factor a as depicted in Fig. 3. Excellent correlation coefficient of 95% was found for the proposed values given in Fig. 3.

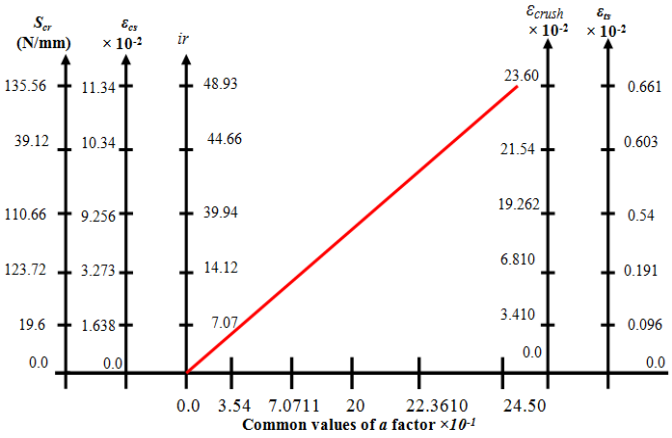

Fig. 3. Common values of proposed nonlinearities.

According to the comparison of the proposed nonlinearities with the experimental data given in Table I, good agreement was obtained.

TABLE I
COMPARISON OF THE PROPOSED NONLINEARITIES WITH SOME EXPERIMENTAL DATA

Proposed/ Experimental value	Proposed value	Experimental value	Aspect ratio	Fiber content %	Proposed model
ir	1.0012	1.18144	1.18	70.00	0.50
	1.3900	1.67	1.20	70.00	1.00
S_{cr}	0.8115	4.95	6.10	80.00	1.00
	0.8684	4.95	5.70	80.00	1.00
	1.2700	4.95	3.90	80.00	1.00
	0.9722	7.00	7.20	80.00	2.00
	1.0938	7.00	6.40	80.00	2.00
ε_{cs}	0.5333	0.0016	0.0030	55.046	0.50
	0.7188	0.0023	0.0032	55.046	1.00
	0.7800	0.0027	0.0035	55.046	1.50
ε_{crush}	0.8556	0.0077	0.0090	40.00	1.60
	0.9636	0.0106	0.0110	40.00	3.00
ε_{ts}	0.9308	0.0001	0.0001	40.00	0.50
	0.9500	0.0001	0.0001	40.00	1.00
	1.00	0.0002	0.0002	40.00	1.50

C. *Nonlinear Finite Element Static Analysis*

Nonlinear behavior is usually used in the analysis of concrete structures due to the cracking of concrete or yielding of steel bars. In the present study, Newton-Raphson approach was used. In this approach, four cases of stiffness matrix determination have been considered, namely, using of initial stiffness matrix for all load increments, considering tangential stiffness method in static analysis, calculating of stiffness matrix in the first iteration of each load increment and determining of stiffness matrix in the second iteration of each load increment. The convergence of the static analysis solution during each load increment is checked with using tolerance of 0.008. Thus the closeness of analysis outputs to the actual results is satisfied as shown in Fig. 4.

Computer program coded in FORTRAN language was prepared to investigate the static analysis of concrete SFRC beam. Present proposed nonlinear novel formulations were used in this program. The flow chart of this analytical procedure is depicted in Fig. 5.

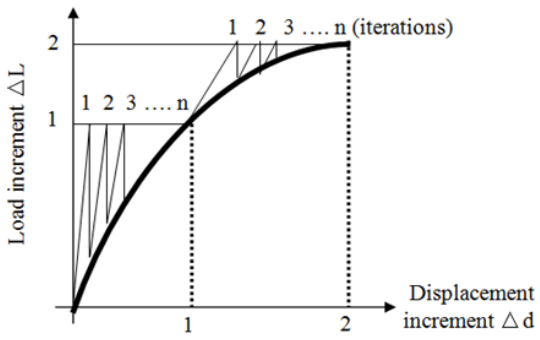

Fig. 4. Newton-Raphson concept.

http://dx.doi.org/10.14500/aro.10041

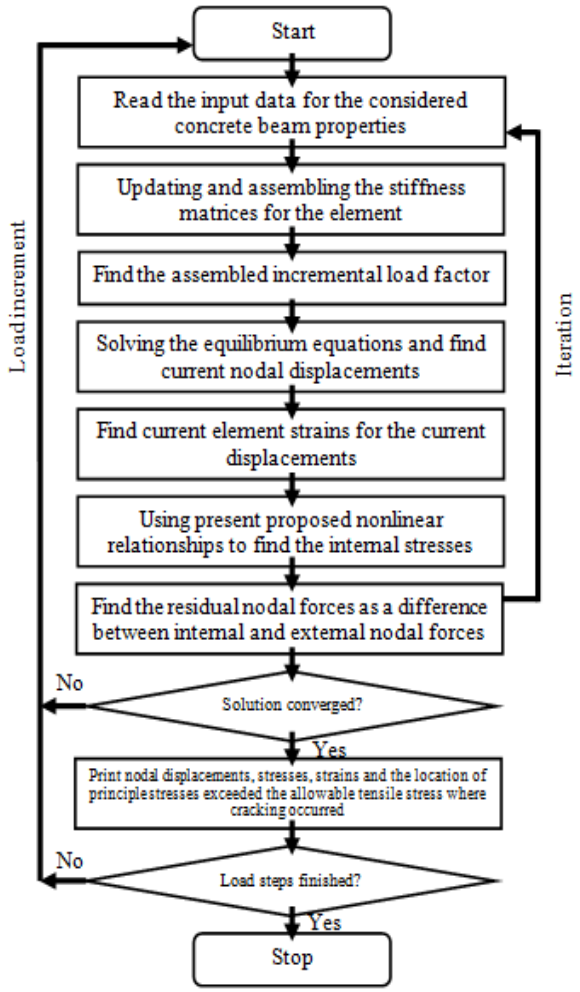

Fig. 5. Outline of present computer program for static analysis of SFRC beam

III. Numerical Applications

Many SFRC beams contain various steel fiber shapes have been considered in the static analysis with using current nonlinear finite element procedure. The validity of the proposed nonlinear models in static analysis outcomes of SFRC beams has been taken into account.

A. SFRC Beam with Square Cross Section and Subjected to a Point Load

A SFRC beam with the geometry, reinforcement and loading given in Fig. 6 was tested by Compione and Mangiavillano (2008). Hooked steel fibers have been used in the preparing of fibrous concrete beam. The characteristics of the beam and the used steel fibers are listed in Table II. Three different effective thicknesses 5mm, 15mm and 25mm for concrete cover were adopted in the flexural test. This beam was considered in present static analysis procedure to check the validity of the proposed nonlinearities and consequently the developed heterosis finite element analysis. Half of the beam was selected in the analysis due to the symmetry of the beam geometry and loading. Two heterosis elements (Fig. 7) with ten concrete strata and two steel bar layers were used to model half of the beam. Four cases of stiffness matrix determinations given in section II-B are used in beam analysis. The outcomes are represented in terms of load-central deflection curves, ultimate loads and failure shape of the beam.

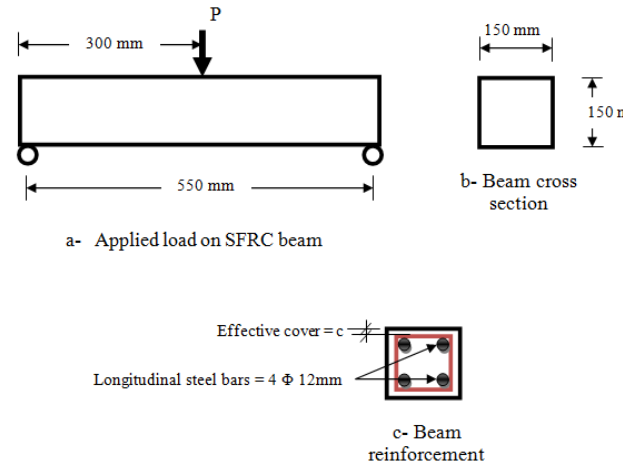

Fig. 6. SFRC beam 1.

TABLE II
Properties of Reinforced Concrete Used for SFRC Beam 1

Compressive strength MPa	36.19
Tensile strength MPa	3.31
Yield stress of steel bars MPa	467
Modulus of Elasticity of steel bars MPa	206000
Fiber length mm	30
Fiber diameter mm	0.5
Fiber aspect ratio	60
Steel fiber content in concrete %	1

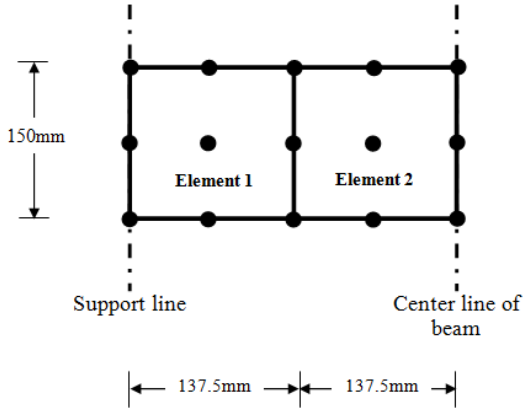

Fig. 7. Finite element mesh of SFRC beam 1.

Present load-displacement curves are compared with the experimental outputs given by Compione and Mangiavillano (2008) as illustrated in Figs. 8–10, good correlation was observed in using stiffness case 2 compared to other cases. This has been proved by determining the average value of ratios of the determined displacement (for each stiffness case) and measured experimental displacement at the ultimate load. In the other words, the ratio which is close to one is the best case.

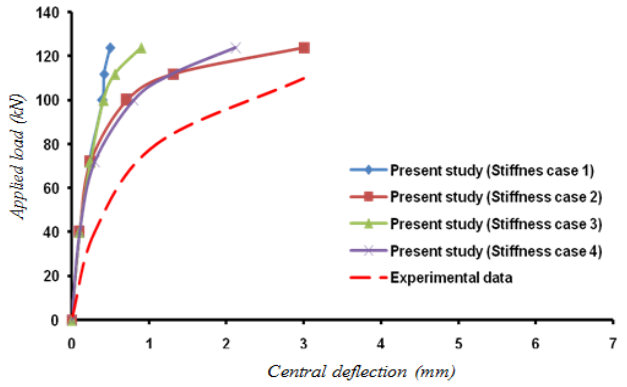

Fig. 8. Load-deflection relationship for SFRC beam 1 with c = 5mm.

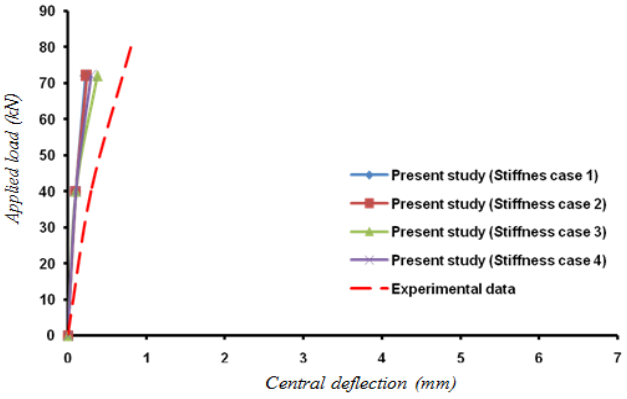

Fig. 9. Load-deflection relationship for SFRC beam 1 with c=15mm.

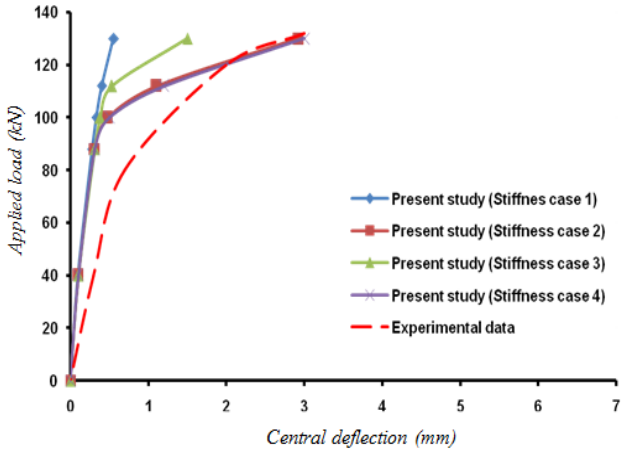

Fig. 10. Load-deflection curve for SFRC beam 1 with c=25mm.

So, according to Table III and Fig. 11, the employment of case 2 gives good results and the calculated displacement value is about 80% of actual magnitude with consideration of three concrete cover values of 5mm, 15mm and 25mm.

TABLE III
DISPLACEMENT ACCOMPANIED WITH THE ULTIMATE LOAD

Effective cover mm	Stiffness case	Displacement (Present study)	Displacement (Experimental result)	Analytical results/Experimental outcomes
5	1	0.5524	3	0.1841
	2	2.924		0.9750
	3	1.50		0.50
	4	3.00		1.00
15	1	0.2243	0.80	0.2804
	2	0.24		0.30
	3	0.375		0.47
	4	0.30		0.3750
25	1	0.50	3	0.17
	2	3.011		1.004
	3	0.90		0.30
	4	2.12		0.71

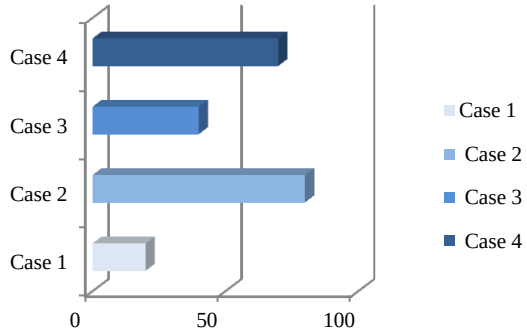

Fig. 11. Compatibility between numerical and experimental outputs for beam 1.

The failure pattern under static loading was also estimated by using present finite element formulations with stiffness case 2 for many load steps as depicted in Fig. 12. With performing comparison between the numerical cracking pattern and actual beam failure from the test (Fig. 13), it was observed that the cracks are concentrated in the region close to the mid-span of the beam which agree with the experimental failure mode.

B. SFRC Beam with Rectangular Cross Section and Subjected to a Point Load

A simply supported SFRC beam (Fig. 14) tested by Swamy and Al-Ta'an (1981) is selected in present analysis. The mechanical properties of the concrete used for the beam is given in Table IV. Crimped steel fibers with the properties listed also in Table IV were used. Due to the symmetrical

http://dx.doi.org/10.14500/aro.10041

geometry and loading of the beam, half of the beam was considered in the analysis adopting three heterosis elements as illustrated in Fig. 15. The results of current analysis and experimental outcomes are given in terms of applied force - central displacement and strains of beam as given in Figs. 16-18.

According to the comparison between numerical and experimental outcomes in these figures, suitable agreement was observed specially by considering stiffness cases 2 and 4 in the present analysis. The difference in analytical outcomes with experimental values in Fig. 16 is attributed to the some approximate concepts in the present finite element analysis such as disregarding the effect of shear stirrups.

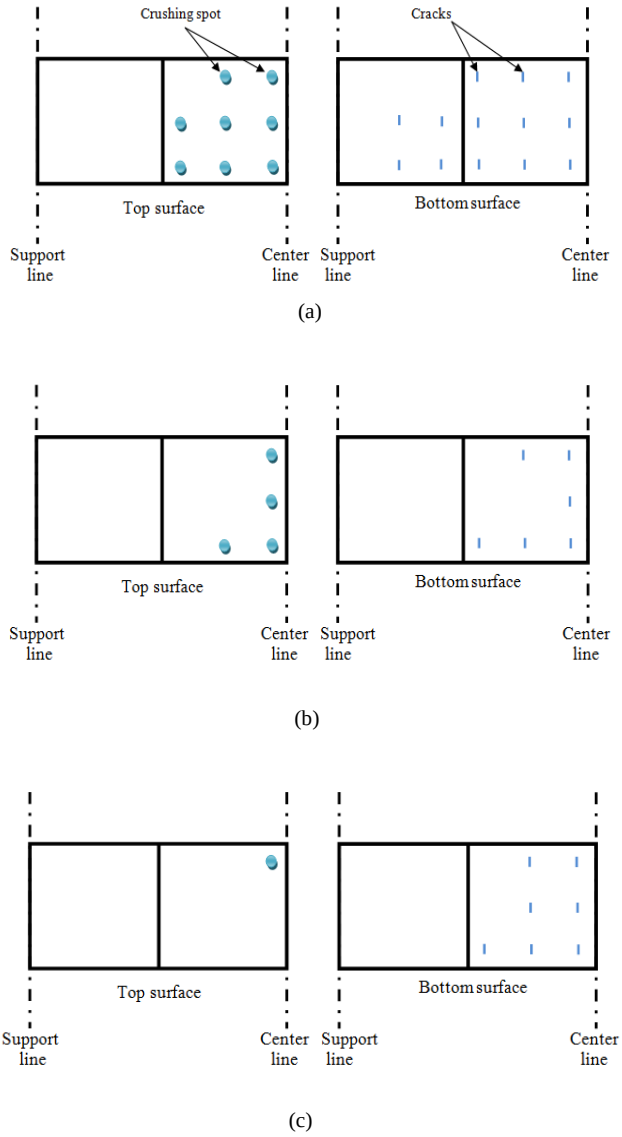

Fig. 12. Failure pattern for SFRC beam using present finite element procedure; (a) Failure at load of 120 kN for beam 1 with c=5mm, (b) Failure at load of 67 kN for beam 1 with c=15mm and (c) Failure at load of 64 kN for beam 1 with c=25mm.

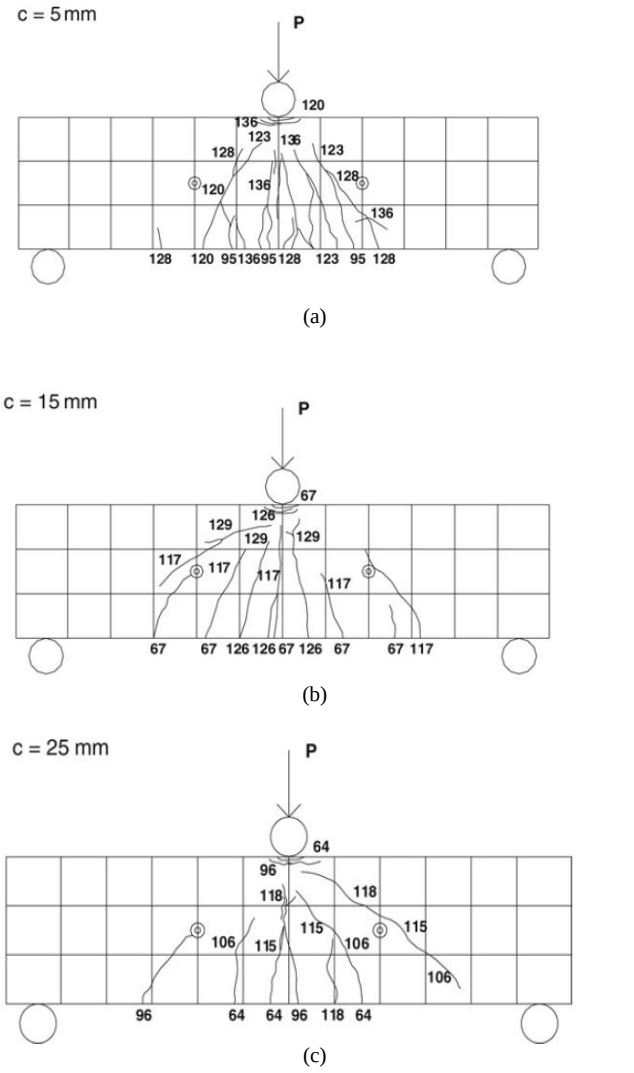

Fig. 13. Experimental failure pattern for SFRC beam 1 (Compione and Mangiavillano, 2008); (a) Failure for beam 1 for applied load 120, (b) Failure at load of 67 kN for beam 1 with c=15mm and (c) Failure for beam 1 for applied load 64 kN.

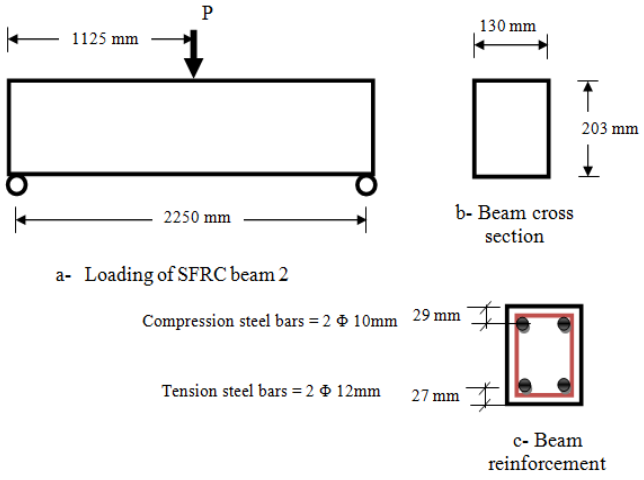

Fig. 14. SFRC beam 2.

TABLE IV
PROPERTIES OF CONCRETE USED FOR SFRC BEAM 2

Compressive strength MPa	28.40
Tensile strength MPa	5.80
Yield stress of steel bars MPa	475
Modulus of Elasticity of concrete MPa	29820
Fiber length mm	50
Fiber diameter mm	0.5
Fiber aspect ratio	100
Steel fiber content in concrete %	1

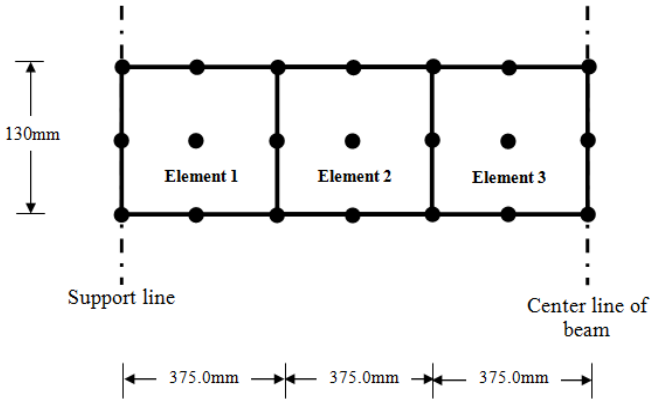

Fig. 15. Finite element mesh of SFRC beam 2.

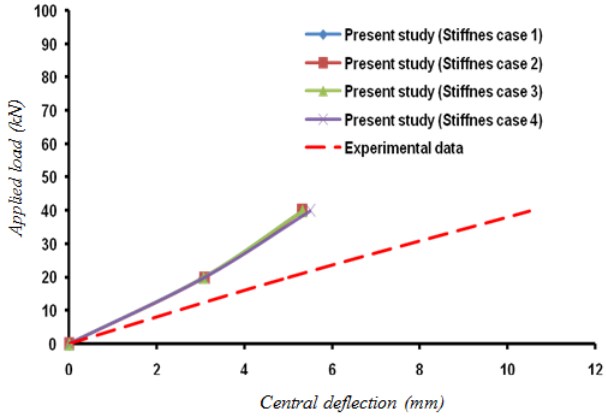

Fig. 16. Load-deflection curve for SFRC beam 2.

C. *SFRC beam with rectangular cross section and subjected to two point forces*

Shallow SFRC beam (Fig. 19) tested by Narayanan and Darwish (1987) was adopted in present finite element analysis. The properties of this concrete beam are given in Table V. Half of the beam was considered in analysis because of the condition of symmetry. Thus, four heterosis elements with ten concrete strata were used to model the half of beam as in Fig. 20. The static performance of the beam is represented in the form of displacement values at specific applied load magnitudes and ultimate applied load values.

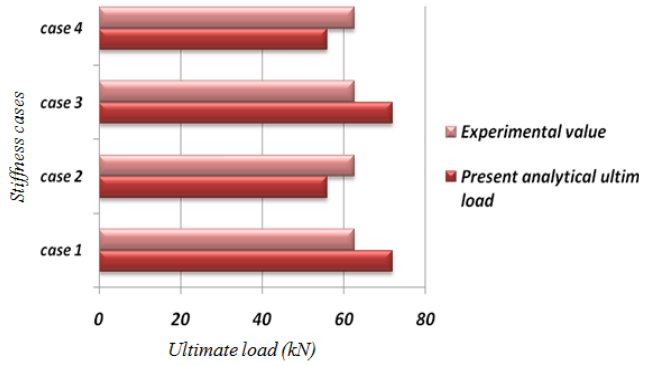

Fig. 17. Ultimate load for SFRC beam 2

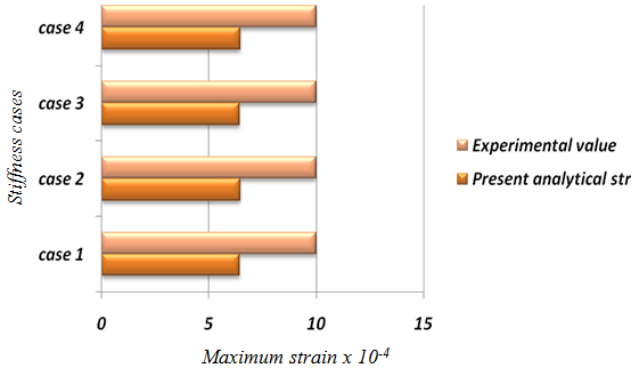

Fig. 18. Maximum longitudinal strains of tension steel bars for SFRC beam 2

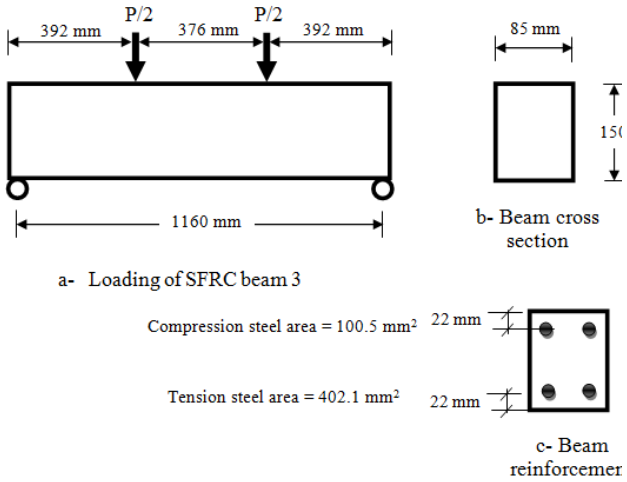

Fig. 19. SFRC beam 3.

http://dx.doi.org/10.14500/aro.10041

TABLE V
PROPERTIES OF REINFORCED CONCRETE USED FOR SFRC BEAM 3

Compressive strength MPa	71.90
Tensile strength MPa	6.03
Yield stress of steel bars MPa	530
Modulus of Elasticity of concrete MPa	29790
Fiber length mm	40
Fiber diameter mm	0.30
Fiber aspect ratio	133
Steel fiber content in concrete %	1

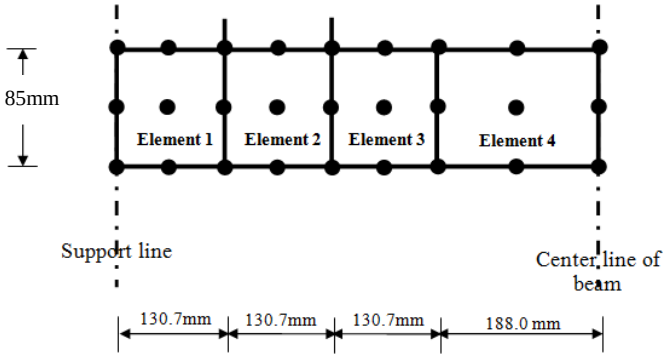

Fig. 20: Finite element mesh of SFRC beam 3.

Present numerical results are compared to the experimental outcomes as shown in Figs. 21-23, good harmony was observed. The adopting of case 4 of stiffness calculation is considered more suitable than other cases especially in determination of displacement values.

Generally, it is observed in the aforementioned results that the stiffness cases 2 and 4 give more reasonable outcomes. The using of tangent stiffness and stiffness in the second iteration is relatively more realistic due to the decreasing of error produced in numerical solution compared to the proposed initial stiffness condition.

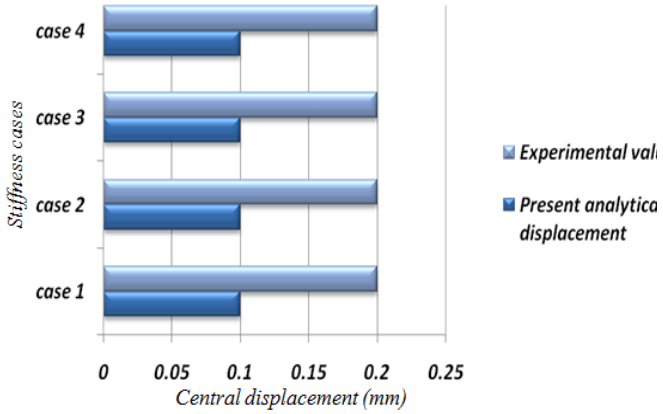

Fig. 21. Central deflection at load step of 12 kN of SFRC beam 3.

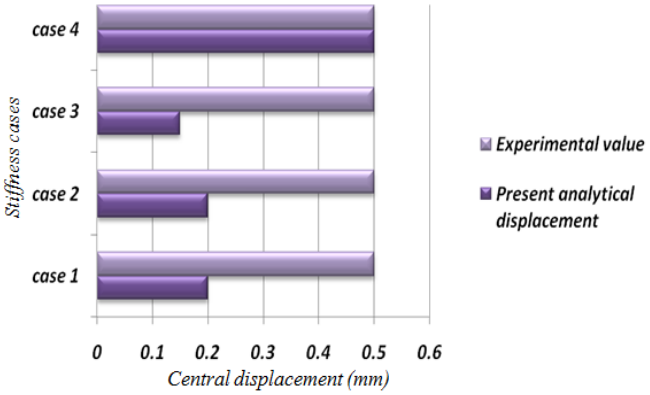

Fig. 22. Central deflection at load step of 20 kN of SFRC beam 3.

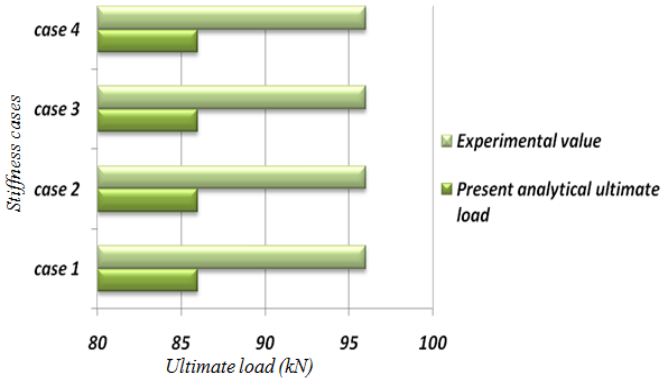

Fig. 23. Ultimate applied load for SFRC beam 3.

IV. CONCLUSIONS

In the present study, new and simple nonlinearities for simulation of SFRC performance were proposed depending on many experimental data. Finite element procedure has been developed for static analysis of SFRC beam based on using the proposed nonlinearities in formulation of the nine nodes heterosis elements. According to the outcomes of the aforementioned applications, it can be concluded that;

1) The proposed models for SFRC behavior are valid for static analysis purpose of SFRC beams that contain many steel fibers shapes and sizes.
2) The best results have been found in present finite element static analysis with considering the tangential stiffness matrix and stiffness matrix in second iteration of the load increment.

REFERENCES

Abdul-Razzak, A.A. and Ali, A.A.M., 2011. Modeling and numerical simulation of high strength fiber reinforced concrete corbels. *Applied Mathematical Modeling*, 35(6), pp.2901-2915.

Abdul-Razzak, A.A. and Ali, A.A.M., 2011. Influence of cracked concrete models on the nonlinear analysis of high strength steel fiber reinforced concrete corbels. *Composite Structures*, 93(9), pp.2277-2287.

Alavizadeh-Farhang, A., 1998. *Plain and steel fiber reinforced concrete beams subjected to combined mechanical and thermal loadings*. M.Sc. Thesis, Department of Structural Engineering, Royal Institute of Technology, Stockholm, Sweden.

Al-Ta'an, S.A. and Ezzadeen, N.A., 1995. Flexural analysis of reinforced fibrous concrete members using finite element method. *Computer and Structures*, 56(6), pp.1065-1072.

ANSYS, 2003. *Swanson Analysis System*. US.

Ashour, S.A., Wafa, F.F. and Kamal, M.I., 2000. Effect of the concrete compressive strength and tensile reinforcement ratio on the flexural behavior of fibrous concrete beams. *Engineering Structures*, 22(9), pp.1133–1146.

Bangash, M.Y.H., 1989. *Concrete and concrete applications*. London, England: Elsevier Science Publishers Ltd.

Bayramov, F., Tasdemir, C. and Tasdemir, M.A., 2004. Optimization of steel fiber reinforced concretes by means of statistical response surface method. *Cement and Concrete Composites*, 26(6), pp.665–675.

Bencardino, F., Rizzuti, L., Spadea, G. and Swamy, R.N., 2010. Experimental evaluation of fiber reinforced concrete fracture properties. *Composites Part B-Engineering*, 41(1), pp.17–24.

Compione, G. and Mangiavillano, M. L., 2008. Fibrous reinforced concrete beams in flexure: Experimental investigation, analytical modeling and design considerations. *Engineering Structures*, 30(11), pp.2970-2980.

Cucchiara, C., La Mendola, L. and Papia, M., 2004. Effectiveness of stirrups and steel fibers as shear reinforcement. *Cement and Concrete Composites*, 26(7), pp.777-786.

Dupont, D., and Vandewalle, L., 2002. *Bending capacity of steel fiber reinforced concrete SFRC beams*. In: *International Congress on Challenges of Concrete Construction*. Dundee, pp.81-90.

Ganesan, N., and Shivananda, K.P., 2002. *Spacing and width of cracks in polymer modified steel fiber reinforced concrete flexural members*. In: International Congress on Challenges of Concrete Construction, Dundee, pp.244-253.

Gopalaratnam, U.S., Shah, S.P., Batson, G.B., Criswell, M.E., Ramaksishran, U., and Wecharatara, M., 1991. Fracture toughness of fiber reinforced concrete. *ACI Materials Journal*, 8(4), pp.339-353.

Hartman, T., 1999. *Steel fiber reinforced concrete*. M.Sc. Thesis, Department of Structural Engineering, Royal Institute of Technology, Stockholm, Sweden.

Hasan, N.H.J., 2002. *Nonlinear finite element analysis of fibrous reinforced concrete slabs*. M.Sc. Thesis, University of Mosul.

Hemmaty, Y., 1998. *Modeling of the shear force transferred between cracks in reinforced concrete structures*. In: *Proceedings of ANSYS Conference*, Vol. 1, Pittsburgh, Pennsylvania.

Hsu, L.S. and Hsu, C.T.T., 1994. Stress–strain behavior of steel-fiber high-strength concrete under compression. *ACI Structural Journal*, 91(4), pp.448-457.

Huyse, L., Hemmaty, Y. and Vandewalle, L., 1994. *Finite element modeling of fiber reinforced concrete beams*. In: *Proceedings of the ANSYS Conference*, Vol. 2, Pittsburgh, Pennsylvania.

Koksal, F., Altun, F., Yigit, I. and Sahin, Y., 2008. Combined effect of silica fume and steel fiber on the mechanical properties of high strength concretes. *Construction and Building Materials*, 22(8), pp.1874–1880.

Kurihara, N., Kunieda, M., Kamada, T., Uchida, Y. and Rokugo, K., 2000. Tension softening diagrams and evaluation of properties of steel fiber reinforced concrete. *Engineering Fracture Mechanics*, 65(2-3), 235-245.

Lim, D.H. and Nawy, E.G., 2005. Behavior of plain and steel-fiber-reinforced high-strength concrete under uniaxial and biaxial compression. *Magazine of Concrete Research*, 57(10), pp.603-610.

Lin, W.T., Huang, R., Lee, C.L. and Hsu, H.M., 2008. Effect of steel fiber on the mechanical properties of cement-based composites containing silica fume. *Journal of Materials Science and Technology*, 6(3), pp.214–221.

Narayanan, R. and Darwish, I.Y.S., 1987. Use of steel fibers as shear reinforcement. *ACI Structural Journal*, 84(3), pp.216-227.

Ocean Heidelberg Cement Group, 1999. *Ocean concrete products, steel fiber reinforcement, working together to build our communities report*.

Paine, K.A., Elliott, K.S. and Paston, C.H., 2002. *Flexural toughness as a measure of shear strength and ductility of prestressed fiber reinforced concrete beams*. In: International Congress on Challenges of Concrete Construction, Dundee, pp.200-212.

Song, P.S. and Hwang, S., 2004. Mechanical properties of high-strength steel fiber reinforced concrete. *Construction and Building Materials*, 18(9), pp.669-673.

Swamy, R.N. and AL-Ta'an, S.A., 1981. Deformation and ultimate strength in flexure of reinforced concrete beams made with steel fiber concrete. *ACI Journal Proceedings*. 78(5), pp.395-405.

Thomas, J. and Ramaswamy, A., 2007. Mechanical properties of steel fiber-reinforced concrete. *ASCE Journal of Materials in Civil Engineering*, 19(5), pp.385-392.